Available online at www.sciencedirect.com
ScienceDirect
Tetrahedron
Tetrahedron 63 (2007) 3515–3527

Furan decorated nucleoside analogues as fluorescent probes: synthesis, photophysical evaluation, and site-specific incorporation

Nicholas J. Greco and Yitzhak Tor*

Department of Chemistry and Biochemistry, University of California, San Diego, MC 0358, La Jolla, CA 92093 0358, USA

Received 16 June 2006; revised 18 January 2007; accepted 18 January 2007
Available online 3 February 2007

Abstract—The synthesis and photophysical evaluation of modified nucleoside analogues in which a five-membered heterocycle (furan, thiophene, oxazole, and thiazole) is attached to the 5-position of 2′-deoxyuridine are reported. The furan-containing derivative is identified as the most promising responsive nucleoside of this family due to its emission quantum efficiency and degree of sensitivity to its microenvironment. The furan moiety was then attached to the 5-position of 2′-deoxycytidine as well as the 8-position of adenosine and guanosine. Photophysical evaluation of these four furan-containing nucleoside analogues reveals distinct differences in the absorption, emission, and quantum efficiency depending upon the class of nucleoside (pyrimidine or purine). Comparing the photophysical properties of all furan-containing nucleosides, identifies the furan thymidine analogue, 5-(fur-2-yl)-2′-deoxyuridine, as the best candidate for use as a responsive fluorescent probe in nucleic acids. 5-(Fur-2-yl)-2′-deoxyuridine was then converted to the corresponding phosphoramidite and site specifically incorporated into DNA oligonucleotides with greater than 88% coupling efficiency. Such furan-modified oligonucleotides form stable duplexes upon hybridization to their complementary DNA strands and display favorable fluorescent features.

1. Introduction

Fluorescence spectroscopy provides biophysicists with incredible opportunities to explore the structure, dynamics, and recognition of biomolecules. Nucleic acids, however, present a challenge since the common pyrimidines and purines are practically non-emissive.[1–9] Adenosine, for example, displays a quantum yield of 0.00005.[8] To remedy this limitation, numerous fluorescent nucleobase analogues have been synthesized and implemented. These probes can be classified into several major families, including: (a) isomorphic base analogues; heterocycles that closely resemble the corresponding natural nucleobases with respect to their overall dimensions, hydrogen bonding face, and ability to form isostructural Watson–Crick (WC) base pairs (Fig. 1a);[10–12] (b) pteridines as purine analogues; intensely fluorescent heterocycles that contain two condensed six-membered rings (Fig. 1b);[13] (c) expanded nucleobases, where the natural bases are extended by conjugation to additional aromatic rings (Fig. 1c);[14–28] (d) chromophoric base analogues, where the natural heterocycle is replaced with a fluorescent aromatic residue (Fig. 1d);[29–38] and (e) conjugated base analogues, where fluorescent aromatic moieties are linked to the natural nucleobases (Fig. 1e).[39–46] Notably, favorable photophysical characteristics are typically associated with significant structural perturbation when compared to the heterocycles found in the native nucleobases.

We have recently initiated a program directed at the design, synthesis, and implementation of new fluorescent isosteric nucleosides. We expect the newly designed analogues to fulfill the following requirements: (a) to maintain high structural similarity to the natural nucleobases and ensure the formation of WC-like base pairs, (b) to display emission at long wavelengths (preferably in the visible range), (c) to retain adequate emission quantum efficiency upon incorporation into an oligonucleotide, and, most importantly, (d) to respond to changes in their microenvironment via marked differences in their basic photophysical parameters.

Our basic design principle relies on conjugating or fusing aromatic five-membered rings to a pyrimidine core. Examination of the photophysical properties of simple conjugated heterocycles reveals intriguing fluorescent properties. Comparing the absorption and emission spectra of benzene[47,48] and furan to that of the corresponding 2-phenylfuran, for example, clearly illustrates the favorable features of the conjugated system (Fig. 2). While benzene and furan have relatively weak absorption bands above 250 nm, the conjugated 2-phenylfuran, under the same experimental conditions,

* Corresponding author. Tel.: +1 858 534 6401; fax: +1 858 534 0202; e-mail: ytor@ucsd.edu

0040–4020/$ - see front matter © 2007 Elsevier Ltd. All rights reserved.
doi:10.1016/j.tet.2007.01.073

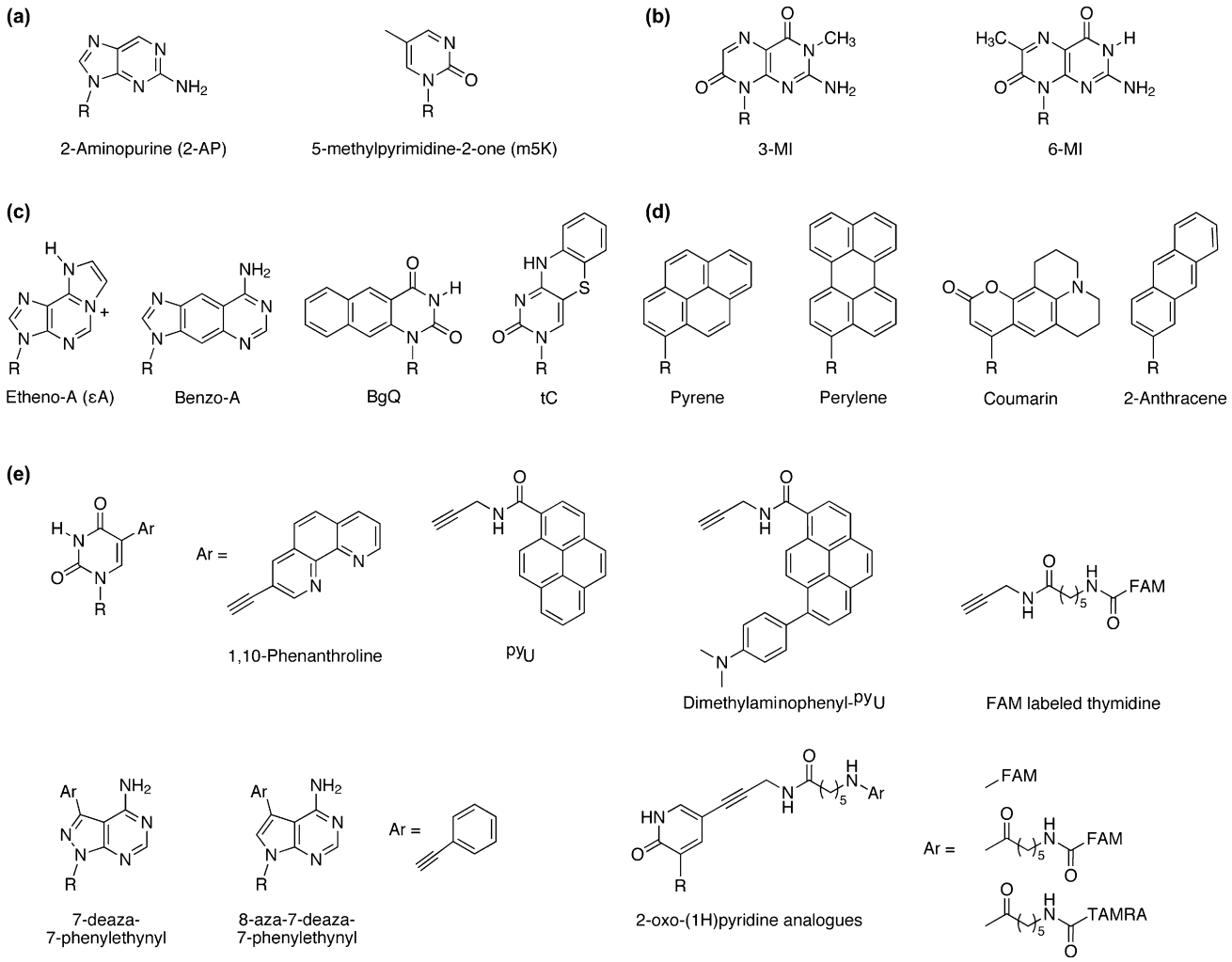

Figure 1. Families of fluorescent nucleoside analogues: (a) isomorphic nucleobases, (b) pteridines, (c) expanded nucleobases, (d) chromophoric nucleobases, and (e) conjugated nucleobases where R=2′-deoxyribose or ribose.

displays an intense absorption around 280 nm (ε=20,000). This is associated with a strong emission band (ϕ_F=0.4) centered around 320 nm, a feature, that is, completely absent in either of the aromatic precursors. We have therefore chosen to explore a series of nucleoside analogues **1**–**4**, where an aromatic five-membered ring is conjugated at either the 5-position of pyrimidines or 8-position of purines (Fig. 3).[49] Here we report the synthesis, photophysical properties, and DNA incorporation of a representative member of this family of fluorescent nucleobase analogues.

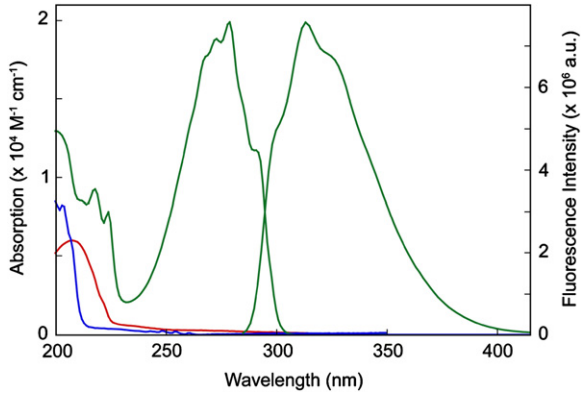

Figure 2. Absorption and emission spectra of furan (red), benzene (blue), and 2-phenylfuran (green) in hexanes (1×10^{-6} M).

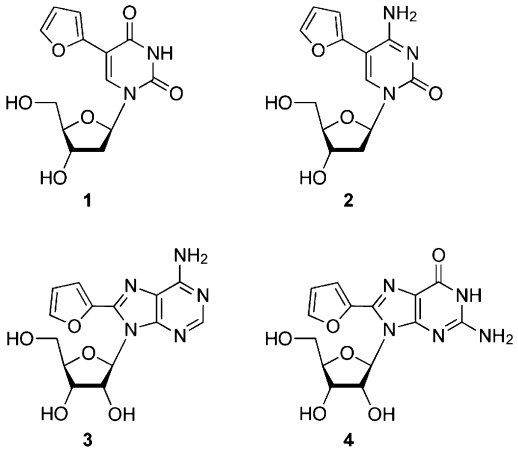

Figure 3. Fluorescent furan-containing nucleoside analogues where a furan moiety is attached to either the 5-position (pyrimidines **1** and **2**) or the 8-position (purines **3** and **4**).

2. Results and discussion

2.1. 5-Substituted deoxyuridine derivatives

We initially probed the virtue of four different five-membered aromatic heterocycles when conjugated to the 5-position of a deoxyuridine core, including furan, thiophene, oxazole, and thiazole. Access to 5-(furyl-2-yl) and 5-(thiophen-2-yl) deoxyuridine analogues was easily achieved under standard Stille coupling conditions, where 2-tributylstannyl furan or thiophene was coupled to 5-iodo-2′-deoxyuridine (Scheme 1).[50] Extension of this procedure to include the oxazole and thiazole analogues through Stille coupling to 5-iodo-2′-deoxyuridine was unsuccessful. Protection of the 3′ and 5′ hydroxyl groups in the 5-iodo-dU precursor was required for obtaining nucleosides **8** and **9** in appropriate quantities.[51] Standard toluyl protection of both hydroxyl groups, followed by Stille coupling afforded nucleosides **8** and **9** in relatively low yields, albeit sufficient for photophysical evaluation.

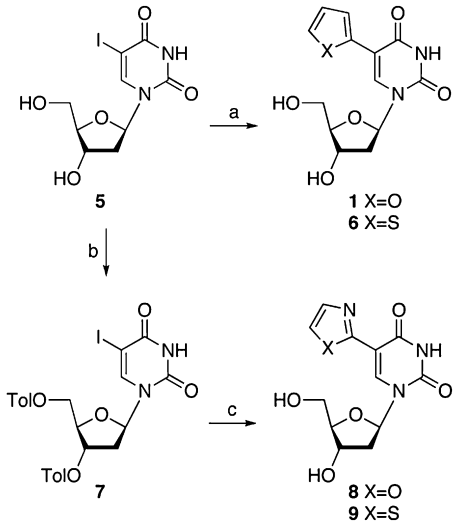

Scheme 1. Reagents: (a) **1**: 2-(tributylstannyl)furan, $PdCl_2(PPh_3)_2$, dioxane, 94%; **6**: 2-(tributylstannyl)thiophene, $PdCl_2(PPh_3)_2$, dioxane, 53%; (b) *p*-toluoyl chloride, pyridine, 85%; (c) **8**: (i) 2-(tributylstannyl)oxazole, $Pd(PPh_3)_4$, toluene; (ii) K_2CO_3, 5% THF/methanol, 10%; **9**: (i) 2-(tributylstannyl)thiazole, $PdCl_2(PPh_3)_2$, dioxane; (ii) K_2CO_3, 5% THF/methanol, 34%.

Rewardingly, all modified nucleosides were found to be emissive. They differ, however, in their quantum yield of emission and sensitivity to their microenvironment polarity (Fig. 4 and Table 1). The absorption spectra of each modified nucleoside reveals a low energy absorption band at ~315 nm for **1**, **6**, and **9** and ~295 nm for **8**, in addition to the typical uridine absorption band at higher energies ~268 nm. The λ_{max} of absorption for all four nucleosides remains practically unchanged upon changing solvent polarity (Table 1). In contrast, the emission profile of the conjugated nucleosides is much more sensitive to the chromophore's microenvironment, with bathochromic (7–36 nm) and hyperchromic (1.0- to 5.6-fold) shifts upon increase in solvent polarity from diethylether to water. In a non-polar environment such as diethylether, all four nucleosides show emission at the higher energy end of the visible range (390–421 nm), with relatively large Stoke shifts (79–101 nm). In water,

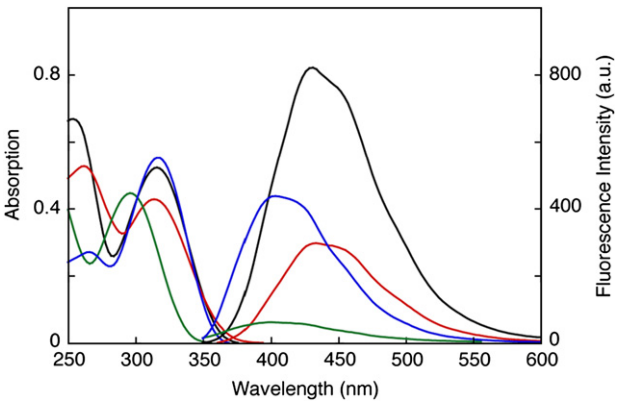

Figure 4. Absorption (5.0×10^{-5} M) and emission (1.0×10^{-5} M) spectra of **1** (black), **6** (red), **8** (green), and **9** (blue) in water.

however, all four nucleosides show emission in the visible range (400–434 nm), with even larger Stoke shifts (88–115 nm). Notably, the quantum efficiency of all four nucleosides is relatively low (0.01–0.03; Table 1). Comparing the quantum efficiencies of the model system, 2-phenylfuran (ϕ_F=0.4), to nucleosides **1**, **6**, **8**, and **9** (ϕ_F=0.03–0.01), reveals ~13- to 40-fold decrease in quantum efficiency. This is not surprising since the quantum efficiency of benzene (ϕ_F=0.07), a component of the model system, is ~500 times more emissive than thymidine (ϕ_F=0.000132).[9] Among all nucleosides tested, the furan-containing analogue **1** displays the most desirable photophysical properties of the four uridine analogues in terms of emission wavelength, quantum yield, and sensitivity to the microenvironment. It has therefore become interest to probe the effect of conjugating a furan moiety onto a cytidine nucleoside, and to explore its effect on the purine nucleus.

2.2. Furan-containing deoxycytidine

Conversion of the furan deoxyuridine analogue **1** to its corresponding deoxycytidine analogue **2** can be accomplished by activation of the 4-position followed by a displacement reaction with ammonia. To facilitate this conversion, the 3′ and 5′ hydroxyl groups were protected as acetate esters. This mode of protection, achieved in quantitative yield by treating **1** with acetic anhydride, was chosen because the use of strongly basic conditions during the aminolysis reaction would also remove the acetate protecting groups, generating the desired free nucleoside. The protected nucleoside **10** was then activated using 2,4,6-triisopropylbenzenesulfonyl chloride in the presence of 4-dimethylaminopyridine and triethylamine. Treatment of the activated nucleoside with ammonium hydroxide and in situ acetate deprotection furnished the desired deoxycytidine nucleoside **2** in 95% yield (Scheme 2).

Table 1. Photophysical data of nucleosides **1**, **6**, **8**, and **9**

Compound	λ_{max} Et_2O (nm)	λ_{max} H_2O (nm)	λ_{em} Et_2O (nm)	λ_{em} H_2O (nm)	I H_2O/ Et_2O	ϕ_F H_2O
1	314	316	395	431	5.6	0.03
6	320	314	421	434	1.6	0.01
8	292	296	390	400	1.0	<0.01
9	318	316	397	404	2.1	<0.01

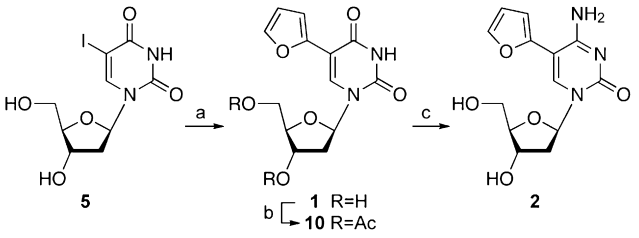

Scheme 2. Reagents: (a) 2-(tributylstannyl)furan, $PdCl_2(PPh_3)_2$, dioxane, 94%; (b) acetic anhydride, pyridine, 99%; (c) (i) 2,4,6-triisopropylbenzenesulfonyl chloride, triethylamine, DMAP, acetonitrile; (ii) ammonium hydroxide, 95%.

The photophysical characteristics of the deoxycytidine analogue **2** were compared with the corresponding precursor deoxyuridine analogue **1**. Both pyrimidine analogues have distinct absorption bands (~315 and ~310 nm for **1** and **2**, respectively) in addition to the natural pyrimidine absorption band at ~260 nm. While nucleoside **1** shows two defined absorption bands of approximately equal intensity at ~260 and ~315 nm, the low energy absorption bands in the cytidine analogue **2** appear as well-defined shoulders in various solvents. As noted above, the absorption of each nucleoside, **1** and **2**, is minimally sensitive to changes in solvent polarity (Fig. 5). The emission spectra, all in the visible range, display much higher sensitivity to changes in the microenvironment. Similar to nucleoside **1**, the cytidine analogue **2** shows bathochromic (12 nm) and hyperchromic (4.4-fold) shifts upon increasing solvent polarity. Note, however, the quantum efficiency of the dC analogue **2** is approximately 3-fold lower than that of the dU analogue **1** (Table 2).

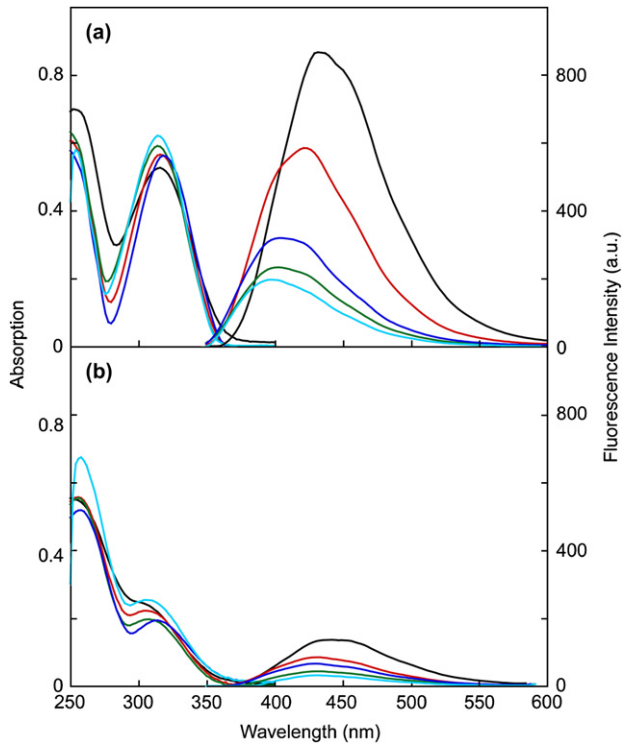

Figure 5. Absorption (5.0×10^{-5} M) and emission (1.0×10^{-5} M) spectra of **1** (a) and **2** (b) in water (black), methanol (red), acetonitrile (green), dichloromethane (dark blue), and ethyl acetate (light blue).

Table 2. Photophysical data of furan nucleosides **1–4**

Compound	λ_{max} EtOAc (nm)	λ_{max} H_2O (nm)	λ_{em} EtOAc (nm)	λ_{em} H_2O (nm)	I H_2O/ EtOAc	ϕ_F H_2O
1	314	316	397	431	4.4	0.03
2	306	310	431	443	4.4	0.01
3	302	304	372	374	1.6	0.69
4	294	294	370	378	2.5	0.57

2.3. Furan-containing purines

The furan-containing purine analogues, **3** and **4**, were prepared in their ribose form,[52] according to previously published synthetic procedures (Scheme 3).[53] Temporary protection of the free hydroxyls as their TMS derivatives, followed by a Stille coupling reaction with 2-(tributylstannyl)furan and standard deprotection using potassium carbonate in methanol afforded the purine analogues **3** and **4** (Scheme 3). Despite the relatively low and unoptimized yields of this synthetic path, sufficient quantities for photophysical studies were easily obtained.

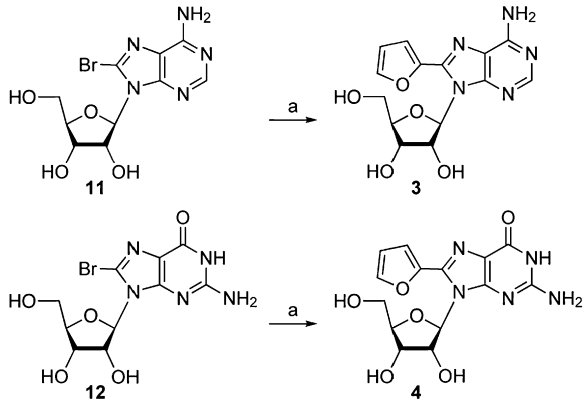

Scheme 3. Reagents: (a) (i) 1,1,1,3,3,3-hexamethyldisilazane, ammonium sulfate, pyridine; (ii) 2-(tributylstannyl)furan, $PdCl_2(PPh_3)_2$, THF; (iii) K_2CO_3, methanol, **3**: 9%; **4**: 10%.

Unlike the pyrimidine analogues, the conjugated purines (**3** and **4**) lack a separate and distinct absorption band, but instead display one major red shifted transition around ~300 nm (Table 2). These absorption bands are largely unaffected by changes in solvent polarity, except in the case of guanosine analogue **4**, where the less polar solvents (dichloromethane and ethyl acetate) show a slightly lower intensity and red shift in comparison to the other more polar solvents (Fig. 6 and Table 2). Intriguingly, the furan-conjugated purines are highly emissive (ϕ_F=0.57 and 0.69 for **3** and **4**, respectively). In contrast to the pyrimidine analogues that typically emit in the visible range, the emission maxima of nucleosides **3** and **4** are centered around 375 nm with an average Stoke shift of 70 and 80 nm, respectively. Somewhat disappointing, however, is the minimal bathochromic effect the purine derivatives display upon increasing solvent polarity, and their limited susceptibility to solvent polarity, with the G derivative **4** being more sensitive than the A analogue **3** (Table 2).

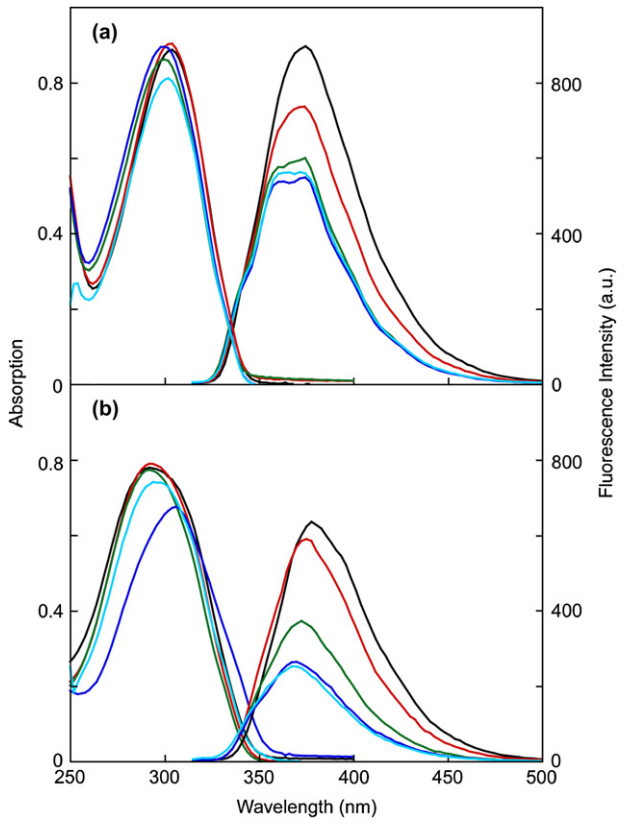

Figure 6. Absorption (5.0×10^{-5} M) and emission (1.0×10^{-5} M) spectra of **3** (a) and **4** (b) in water (black), methanol (red), acetonitrile (green), dichloromethane (dark blue), and ethyl acetate (light blue).

2.4. Temperature effect on emission of furan-containing nucleosides

Inspecting the structure of the four furan-containing nucleosides **1**–**4** suggests that their emission is likely to be temperature dependent. Indeed, all nucleosides display a significant hypochromic effect when their spectra are taken as function of increasing temperatures (Fig. 7). The emission bands of nucleosides **1**, **2**, and **4** display significant susceptibility to increasing temperatures, while the A analogue **3** is affected to a lesser degree. Importantly, this temperature dependent behavior is completely reversible and therefore does not reflect any heat induced chemical transformation. The

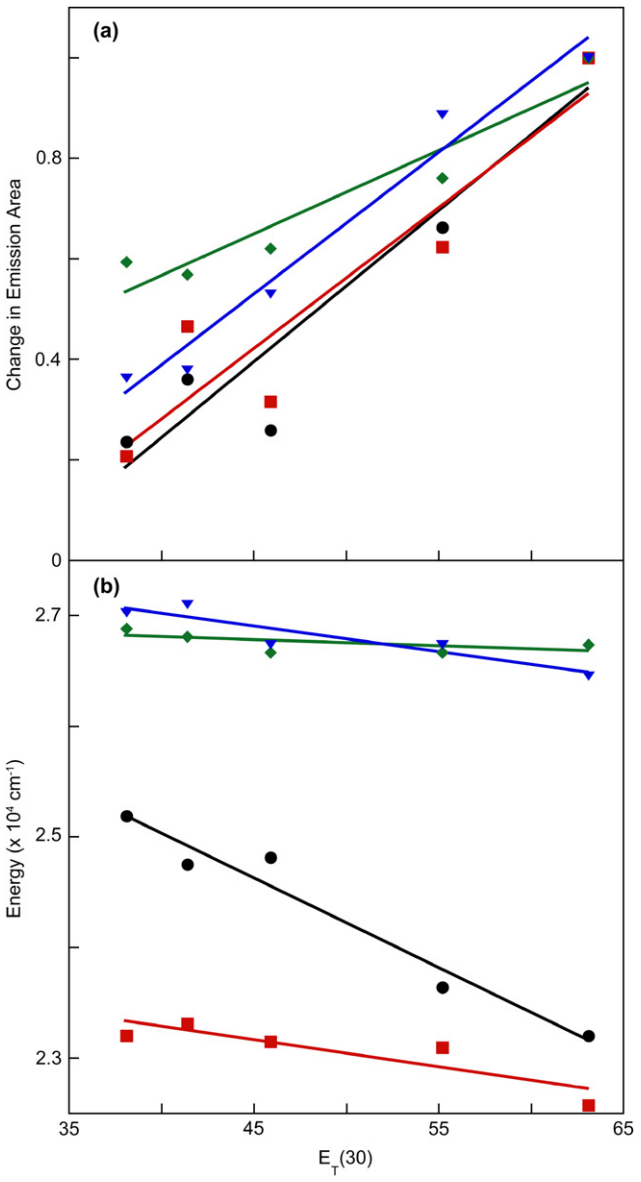

Figure 8. (a) Relationship between change in emission area and microenvironment polarity. (b) Relationship between emission energy and microenvironment polarity. $E_T(30)$ values were experimentally determined for each solvent using Reichardt's salt. For both (a) and (b) **1** (black circles), **2** (red squares), **3** (green diamonds), and **4** (blue triangles).

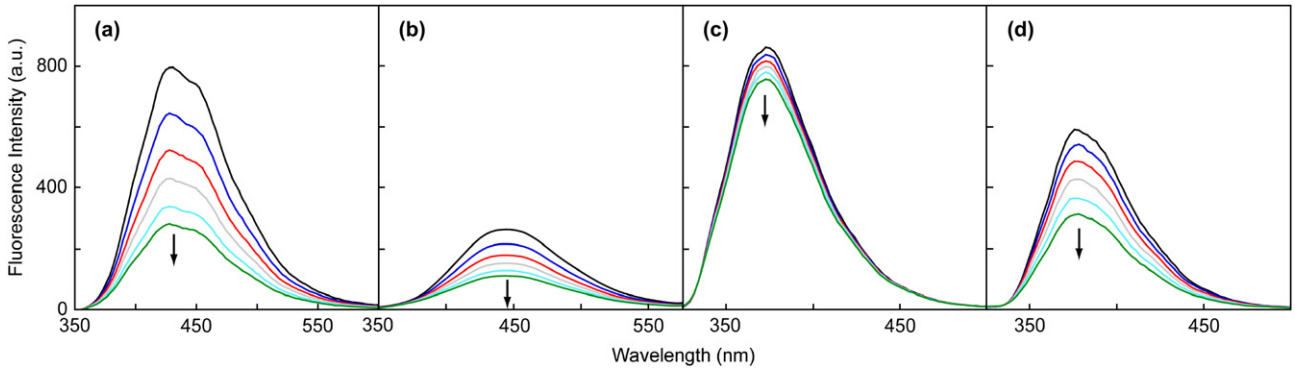

Figure 7. Steady-state emission spectra of **1** (a) 1.0×10^{-5} M, **2** (b) 1.0×10^{-5} M, **3** (c) 1.0×10^{-6} M, and **4** (d) 1.0×10^{-6} M at various temperatures (°C): 25 (black), 35 (dark blue), 45 (red), 55 (gray), 65 (light blue), and 75 (green).

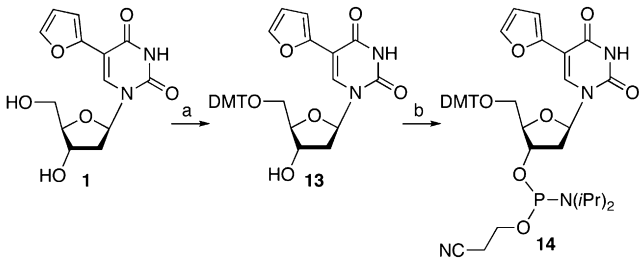

Scheme 4. Reagents: (a) 4,4′-dimethoxytrityl chloride, pyridine, Et_3N, 71%; (b) $(i\text{-}Pr_2N)_2POCH_2CH_2CN$, 1*H*-tetrazole, CH_3CN, 65%.

15 5' – GCG – ATG – **X**GT – AGC – G – 3'
16 5' – CGC – TAC – ACA – TCG – C – 3'
17 5' – GCG – ATG – TGT – AGC – G – 3'

Figure 9. Synthesized oligonucleotides where X=**1**.

sensitivity of the emission quantum yield to temperature is thought to arise from the relatively low barrier for rotation around the furan–pyrimidine/purine single bond that conjugates the two heterocycles. Thermal population of non-radiative decay pathways hence lowers the emission quantum yield at elevated temperatures.

2.5. Selecting a favorable nucleoside for DNA incorporation

Evaluation of all four nucleosides is necessary for the selection of the most responsive probe. As discussed above, absorption bands of all four nucleosides remain largely unaffected by changes in solvent polarity (Table 2), whereas changes in the emission spectra with increasing polarity are seen for all four nucleosides. A graphical comparison of the bathochromic and hyperchromic shifts that take place when the polarity of the microenvironment is increased is given in Figure 8. Plotting the emission area versus $E_T(30)$ values[54] illustrates that all four nucleosides undergo a dramatic hyperchromic shift, as denoted by the positive slope. The slope and ending point suggest that nucleosides **1** and **2** are the most responsive (hyperchromic), followed closely by nucleoside **3** (Fig. 8a). Graphing the emission energy versus $E_T(30)$ values clearly shows that nucleoside **1** experiences the largest bathochromic shift of all four nucleosides upon increasing solvent polarity (Fig. 8b). In contrast, nucleosides **2**, **3**, and **4** all show very shallow dependency on solvent polarity. It is also apparent that the furan-conjugated purines exhibit relatively insensitive emission at significantly higher energies compared to the conjugated pyrimidines. Photophysically, nucleoside **1** is the most responsive nucleoside of the entire family and was therefore selected for site-specific incorporation into oligonucleotides.

2.6. Synthesis and characterization of modified oligonucleotides

Standard solid-phase oligonucleotide synthesis requires 5′-protected and 3′-activated building blocks. Preparation of the required phosphoramidite **14** was achieved through standard 5′-OH protection of nucleoside **1** with 4,4′-dimethoxytrityl chloride in the presence of triethylamine and pyridine (Scheme 4). The 3′-OH was then phosphitylated under standard conditions, resulting in the required modified building block for DNA oligonucleotide synthesis.

Phosphoramidite **14** was used for the synthesis of the singly modified DNA oligonucleotide **15** (Fig. 9), with an unoptimized coupling efficiency of >88% (see Section 4). The fully deprotected oligonucleotide was purified using polyacrylamide gel electrophoresis. Characterization of the modified oligonucleotide **15** was accomplished by MALDI-TOF mass spectrometry. The mass of the purified oligonucleotide **15** was observed to be 4081.98; in good agreement

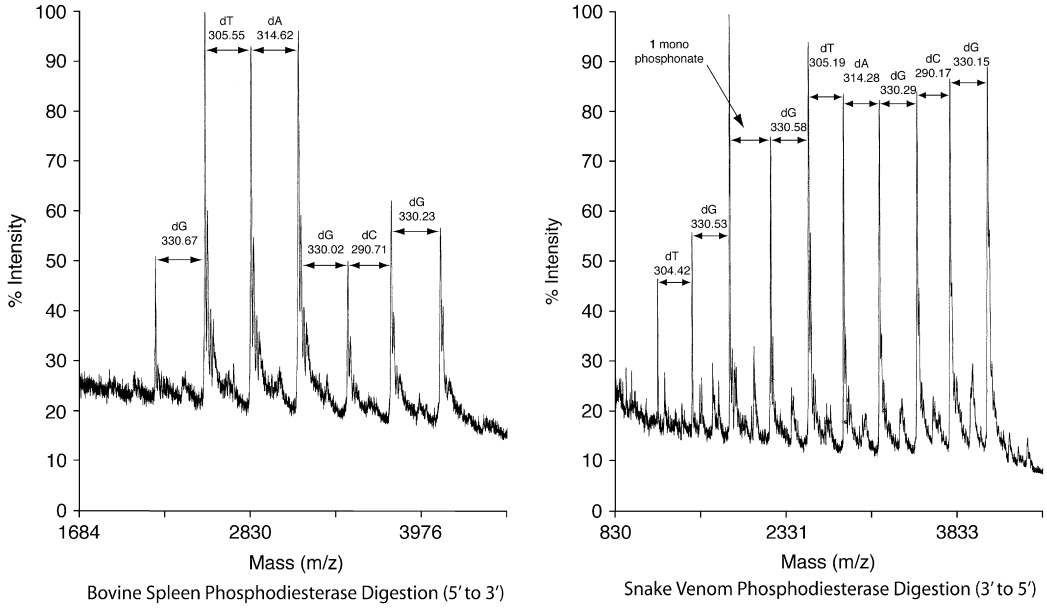

Figure 10. MALDI-monitored digestion of oligonucleotide **15**. Bovine spleen phosphodiesterase (bsp), cleaving in the 5′ to 3′ direction, identifies the first six bases in oligonucleotide **15**, while snake venom phosphodiesterase (svp), cleaving in the 3′ to 5′ direction, identifies nine nucleotides in sequence, including a two nucleotide overlap with the bsp digestion and identification of incorporated nucleotide **1** (see Section 4).

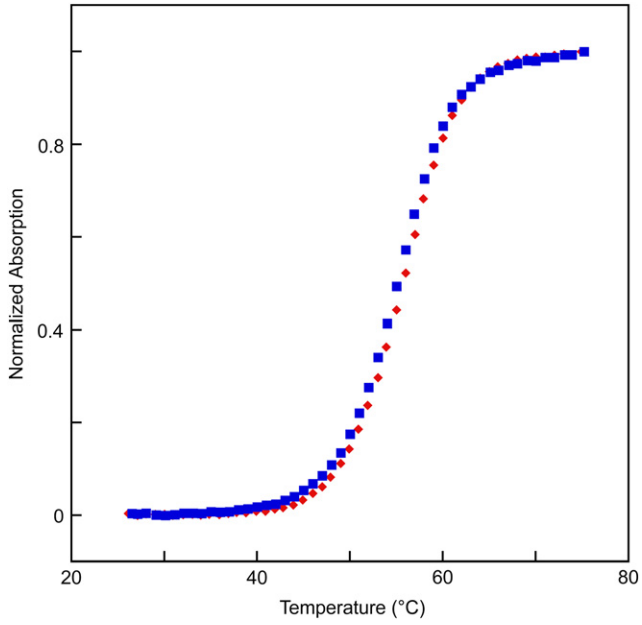

Figure 11. Thermal denaturation curve of modified duplex (**15**·**16**, red diamonds) and unmodified control duplex (**16**·**17**, blue squares) at 1.0×10^{-6} M.

with the calculated mass of 4081.59. Enzymatic digestion experiments, monitored by MALDI-TOF mass spectrometry, using bovine spleen and snake venom phosphodiesterases, clearly confirmed the sequence of the modified oligonucleotide (Fig. 10). These convenient experiments also verified the exact incorporation position of the modified nucleoside and demonstrated that no chemical modification of nucleoside **1** occurred during the numerous coupling, capping, and oxidation steps involved in solid-phase DNA synthesis (Fig. 10). It is worth noting that the singly modified oligonucleotide **15** forms a stable duplex with its perfect complement. Comparing the thermal denaturation curves of the modified duplex **15**·**16** with that of the unmodified duplex **16**·**17** shows that the presence of the modified nucleoside does not significantly affect duplex stability (Fig. 11).

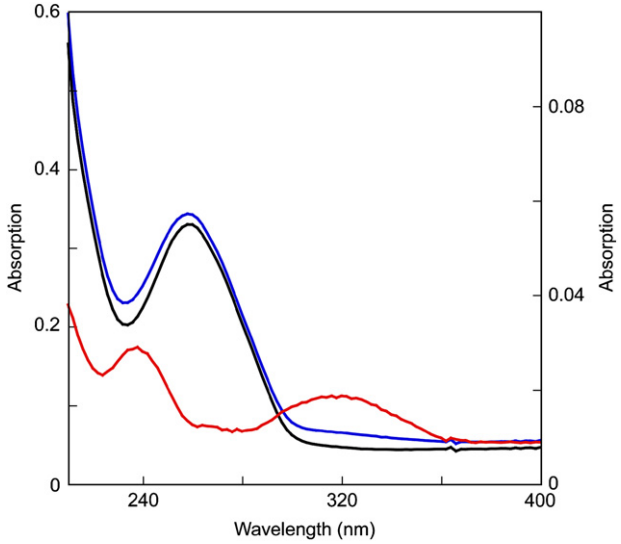

Figure 12. Absorption spectra of oligonucleotide duplexes **15**·**16** (blue) and **16**·**17** (black) at 1.0×10^{-6} M and the subtraction of oligonucleotide duplexes, **15**·**16**–**16**·**17** (red).

Absorption spectra of modified duplex **15**·**16** in comparison with the unmodified duplex **16**·**17** reveal normal absorption bands at 260 nm, but more importantly show a small intensity difference in the 315 nm range (Fig. 12). Subtraction of these two absorption spectra, their nucleoside composition being identical except for the modified nucleoside **1** in duplex **15**·**16**, clearly reveals the second absorption band (~315 nm) of nucleoside **1** (Fig. 12). The λ_{max} of absorption for nucleoside **1** is relatively unchanged upon incorporation into an oligonucleotide. Importantly, nucleoside **1** retains its wavelength of emission upon incorporation into an oligonucleotide. Upon excitation at 320 nm, emission is observed at ~430 nm, as previously seen for nucleoside **1**. The emission curve of oligonucleotide **15** is sharper than the one observed for the free nucleoside in solution and lacks the fine structure observed for nucleoside **1** (comparison of Fig. 13 to Fig. 4). As expected, the furan-containing nucleoside **1** retains its

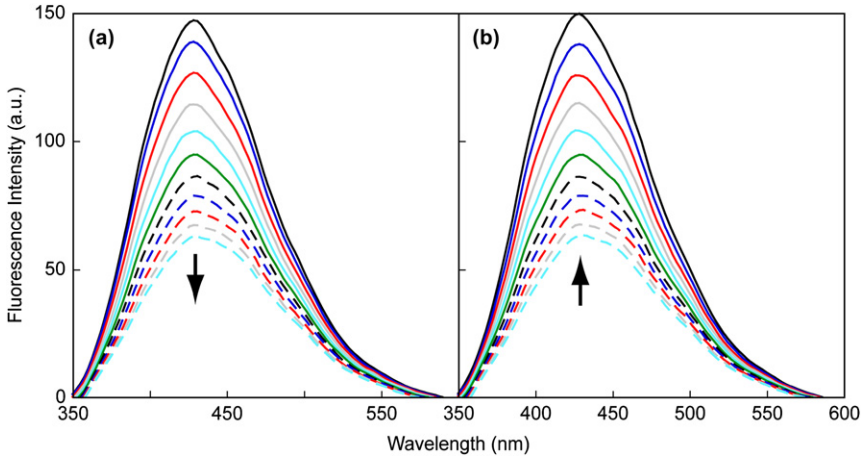

Figure 13. Steady-state emission scans of **15** (1.0×10^{-6} M) at various temperatures (°C) (a) increasing temperature, (b) decreasing temperature: 25 (solid black), 30 (solid dark blue), 35 (solid red), 40 (solid gray), 45 (solid light blue), 50 (solid green), 55 (dashed black), 60 (dashed dark blue), 65 (dashed red), 70 (dashed gray), and 75 (dashed light blue).

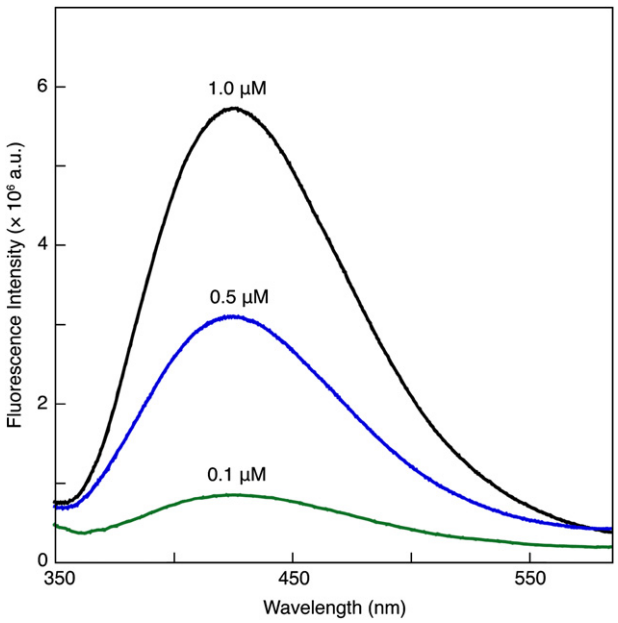

Figure 14. Steady-state fluorescence spectra of oligonucleotide **15** at various concentrations.

reversible temperature sensitive emission after incorporation into an oligonucleotide (Fig. 13).

2.7. Detection limit of single stranded oligonucleotide 15

Quantum efficiency, as noted in Section 1, is of significance in designing and utilizing fluorescent nucleosides as probes for biological systems. Significant decrease in quantum efficiency upon incorporation of a fluorescent nucleoside into RNA/DNA oligonucleotide is a common phenomenon.[10,13,55] Thus, the absolute quantum efficiency of a free nucleoside represents only one facet of this important issue. To experimentally determine the workable concentration window of a fluorescent singly modified oligonucleotide that contains nucleoside **1**, we have measured the emission of oligonucleotide **15** at increasing dilutions. Despite the relatively low quantum efficiency of nucleoside **1** (ϕ_F=0.03), sound emission signals with excellent signal-to-noise ratios are observed at concentrations as low as 100 nM (Fig. 14).[56] As this represents a very common concentration range for many biophysical assays, nucleoside **1** can be of great of experimental utility.

3. Summary

Conjugating a furan ring to the 5-position of the pyrimidines (Fig. 15) and 8-position in the purines provides a family of fluorescent nucleobase analogues. All conjugated nucleosides are emissive, with the pyrimidines emitting in the visible range (400–440 nm) while the purines emit at higher energies (375 nm). Analysis of the solvatochromic behavior of these fluorophores identifies the conjugated dU derivative as the most promising nucleobase for uses in biophysical assays due to the sensitivity of its emission to solvent polarity. Specifically, the furan-conjugated dU derivative **1** exhibits strong visible emission in aqueous environments (λ_{em} 430 nm, ϕ_F=0.03) and significantly weaker emission in apolar media (λ_{em} ~400 nm, ϕ_F ~0.005). A furan-modified oligonucleotide forms stable duplexes with its perfect complement, and importantly retains its absorption (~320 nm) and emission properties (λ_{em} 430 nm). These observations are of significance since useful emissive T/U derivatives are scarce and the trivial synthesis of this nucleoside makes it easily accessible to the biophysical community.

4. Experimental

4.1. General

All chemicals were obtained from commercial suppliers and used without further purification unless otherwise specified. Anhydrous pyridine and acetonitrile were obtained from Fluka. Anhydrous dioxane and triethylamine were obtained from Acros. Anhydrous toluene and tetrahydrofuran were obtained using a two-column purification system (Glasscontour System, Irvine, CA). Analytical thin-layer chromatography was performed on pre-coated silica gel aluminum-backed plates (Kieselgel 60 F_{254}, E. Merck & Co., Germany). Flash chromatography was performed using silica gel (230–400 mesh) from E.M. Science or Silicycle. NMR solvents were purchased from Cambridge Isotope Laboratories (Andover, MA). All NMR spectra were recorded on a Varian Mercury 400 MHz instrument with chemical shifts reported relative to residual deuterated solvent peaks. Chemical shifts (δ) are reported in parts per million (ppm); multiplicities are indicated by s (singlet), d (doublet), t (triplet), q (quartet), dd (doublet of doublet), td (triplet of doublet), or m (multiplet); coupling constants (J) are reported in Hertz. Mass spectra were recorded at the UCSD Mass Spectrometry Facility, utilizing either a LCQDECA (Finnigan) ESI with a quadrupole ion trap or a MAT900XL (ThermoFinnigan) FAB double focusing mass

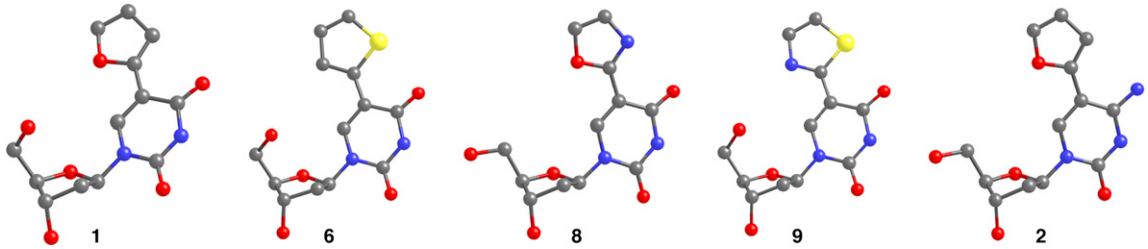

Figure 15. X-ray structures of nucleosides **1**, **6**, **8**, **9**, and **2** with hydrogen and solvent atoms omitted for clarity.

spectrometer. UV–visible experiments were carried out at ambient temperature in a quartz micro cell with a path length of 1.0 cm (Hellma GmbH & Co. KG, Müllheim, Germany) on a Hewlett Packard 8452A or 8453 diode array spectrometer. Steady-state fluorescence experiments were carried out at ambient temperature in a micro fluorescence cell with a path length of 1.0 cm (Hellma GmbH & Co. KG, Müllheim, Germany) on a Perkin–Elmer LS 50B luminescence spectrometer (Figs. 4–7 and 13) or a Horiba fluoromax-3 luminescence spectrometer (Figs. 2 and 14).

4.1.1. 5-(Fur-2-yl)-2′-deoxyuridine (1). To a suspension of **5** (520 mg, 1.47 mmol) and dichlorobis(triphenylphosphine)Pd(II) (21 mg, 0.03 mmol) in anhydrous dioxane (40 ml) was added 2-(tributylstannyl)furan (2 ml, 2.3 g, 6.35 mmol). The suspension was heated to 90 °C under argon for 2 h, cooled, and filtered through Celite 545. The solvent was removed under reduced pressure where the resulting oil was triturated with hexanes (3×) to produce a solid. The resulting solid was taken up in a minimum of hot solvent (1/1 methanol/chloroform) and precipitated from hexanes. Product: white solid (407.7 mg, 1.39 mmol, 94% yield). ^{1}H NMR (400 MHz, DMSO-d_6): δ 11.63 (s, NH, 1H), 8.33 (s, H-6, 1H), 7.62 (s, H-5″, 1H), 6.86 (d, J=2.8 Hz, H-3″, 1H), 6.52 (m, H-4″, 1H), 6.22 (t, J=6.6 Hz, H-1′, 1H), 5.27 (d, J=4.4 Hz, 3′-OH, 1H), 5.08 (t, J=4.4 Hz, 5′-OH, 1H), 4.28 (m, H-3′, 1H), 3.84 (m, H-4′, 1H), 3.61 (m, H-5′, 2H), 2.18 (t, J=5.4 Hz, H-2′, 2H); ^{13}C NMR (100 MHz, DMSO-d_6): δ 160.1 (C-4), 149.4 (C-2), 146.5 (C-2″), 141.5 (C-5″), 134.7 (C-6), 111.6 (C-4″), 107.9 (C-3″), 105.6 (C-5), 87.6 (C-4′), 84.7 (C-1′), 70.4 (C-3′), 61.1 (C-5′), 40.1 (C-2′); HR-FAB calcd for $C_{13}H_{15}N_2O_6$ [M+H]$^+$ 295.0925, found 295.0928; UV (buffer) λ_{max}=316 nm (ε=11,000), ε_{260}=13,000.

4.1.2. 5-(Thiophen-2-yl)-2′-deoxyuridine (6). To a suspension of **5** (521 mg, 1.47 mmol) and dichlorobis(triphenylphosphine)Pd(II) (20 mg, 0.028 mmol) in anhydrous dioxane (40 ml) was added 2-(tributylstannyl)thiophene (2.5 ml, 2.9 g, 7.9 mmol). The suspension was heated to 95 °C under argon for 5 h, cooled, and filtered through Celite 545. The solvent was removed under reduced pressure and the resulting oil was triturated with hexanes (3×) to produce a solid. The resulting solid was taken up in a minimum of hot solvent (1/1 methanol/chloroform) and precipitated from hexanes. Product: white solid (242 mg, 0.779 mmol, 53% yield). ^{1}H NMR (400 MHz, DMSO-d_6): δ 11.7 (s, NH, 1H), 8.57 (s, H-6, 1H), 7.45 (d, J=5.2 Hz, H-5″, 1H), 7.40 (d, J=3.2 Hz, H-3″, 1H), 7.05 (t, J=4.4 Hz, H-4″, 1H), 6.22 (t, J=6.2 Hz, H-1′, 1H), 5.28 (m, 5′-OH and 3′-OH, 2H), 4.31 (m, H-3′, 1H), 3.85 (m, H-4′, 1H), 3.66 (m, H-5′, 2H), 2.21 (m, H-2′, 2H); ^{13}C NMR (100 MHz, DMSO-d_6): δ 161.3 (C-4), 149.4 (C-2), 135.7 (C-6), 134.0 (C-2″), 126.4, 125.7, and 122.5 (C-3″, C-4″, and C-5″), 108.3 (C-5), 87.6 (C-4′), 84.8 (C-1′), 70.0 (C-3′), 60.9 (C-5′), 40.4 (C-2′); HR-FAB calcd for $C_{13}H_{15}N_2O_5S$ [M+H]$^+$ 311.0696, found 311.0701; UV (buffer) λ_{max}=314 nm (ε=9000).

4.1.3. 3′,5′-Di-*O*-*p*-toluoyl-5-iodo-2′-deoxyuridine (7). Anhydrous pyridine (5 ml) was added to **5** (1.00 g, 2.82 mmol) and stirred under argon atmosphere until all starting material was dissolved. The solution was cooled to 0 °C and *p*-toluoyl chloride (785 μl, 918 mg, 5.94 mmol) was added dropwise. Reaction was allowed to warm to room temperature and stirred under argon overnight. Water was added to the reaction solution and the precipitate filtered off. Resulting solid was washed with cold water, cold ethanol, and then cold ether. Product: white solid (1.42 g, 2.41 mmol, 85% yield). ^{1}H NMR (400 MHz, DMSO-d_6): δ 11.76 (s, NH, 1H), 8.09 (s, H-6, 1H), 7.90 (t, J=7.8 Hz, Tol, 4H), 7.34 (t, J=8.8 Hz, Tol, 4H), 6.22 (t, J=7.0 Hz, H-1′, 1H), 5.57–5.56 (m, H-3′, 1H), 4.60 (d, J=4.8 Hz, H-5′, 2H), 4.52–4.49 (m, H-4′, 1H), 2.67–2.60 (m, H-2′, 2H), 2.39 (s, Tol-CH$_3$, 3H), 2.38 (s, Tol-CH$_3$, 3H); ^{13}C NMR (100 MHz, DMSO-d_6): δ 165.5 (Tol-carbonyl), 165.2 (Tol-carbonyl), 160.4 (C-4), 150.0 (C-2), 144.6 (C-6), 144.1 (Tol-C-4), 143.9 (Tol-C-4), 129.4 (Tol-C-2, 3, 5, and 6), 126.5 (Tol-C-1), 85.3 (C-1′), 81.5 (C-4′), 74.5 (C-3′), 70.1 (C-5), 64.2 (C-5′), 36.4 (C-2′), 21.2 (Tol-CH$_3$); ESI-MS calcd for $C_{25}H_{23}IN_2NaO_7$ [M+Na]$^+$ 613.04, found 612.97.

4.1.4. 5-(Oxazol-2-yl)-2′-deoxyuridine (8). To a solution of **7** (98 mg, 0.17 mmol) and tetrakis(triphenylphosphine)Pd(0) (20 mg, 0.017 mmol) in anhydrous toluene (3 ml) was added 2-(tributylstannyl)oxazole (106 μl, 181 mg, 0.506 mmol). The solution was refluxed under argon for 8 h, cooled, and the solvent removed under reduced pressure. The resulting solid was taken up in 20% methanol/chloroform and run through a silica plug where the fractions were collected. Those containing the desired product (fluorescent spot) were consolidated, solvent evaporated under reduced pressure, and resulting solid was taken up in 5% THF/methanol (3 ml) and K_2CO_3 (23 mg, 0.17 mmol) was added. The suspension was stirred at rt for 12 h. The solvent was removed under reduced pressure and product was isolated by flash chromatography (85/15 chloroform/methanol). Resulting solid was triturated with hexanes. Product: white solid (5 mg, 0.02 mmol, 10% yield). ^{1}H NMR (400 MHz, DMSO-d_6): δ 11.65 (s, NH, 1H), 8.58 (s, H-6, 1H), 8.11 (s, H-5″, 1H), 7.26 (s, H-4″, 1H), 6.17 (t, J=6.6 Hz, H-1′, 1H), 5.24 (d, J=3.6 Hz, 3′-OH, 1H), 5.00 (t, J=4.6 Hz, 5′-OH, 1H), 4.25 (m, H-3′, 1H), 3.85 (m, H-4′, 1H), 3.58 (m, H-5′, 2H), 2.19 (m, H-2′, 2H); ^{13}C NMR (100 MHz, DMSO-d_6): δ 159.6 (C-4), 156.6 (C-2″), 149.6 (C-2), 142.1 (C-6), 139.6 (C-5″), 127.7 (C-4″), 102.9 (C-5), 87.8 (C-4′), 85.2 (C-1′), 70.3 (C-3′), 61.0 (C-5′), 40.3 (C-2′); ESI-MS calcd for $C_{12}H_{13}N_3NaO_6$ [M+Na]$^+$ 318.07, found 317.99; UV (buffer) λ_{max}=296 nm (ε=10,000).

4.1.5. 5-(Thiazol-2-yl)-2′-deoxyuridine (9). To a solution of **7** (104 mg, 0.176 mmol) and dichlorobis(triphenylphosphine)Pd(II) (24 mg, 0.033 mmol) in anhydrous dioxane (3 ml) was added 2-(tributylstannyl)thiazole (160 μl, 190 mg, 0.509 mmol). The solution was refluxed at 90 °C under argon for 20 h, cooled, and the solvent was removed under reduced pressure. The resulting solid was triturated with methanol. The precipitate was taken up in 5% THF/methanol (3 ml) and K_2CO_3 (33 mg, 0.24 mmol) was added. The suspension was stirred at rt for 24 h. The solvent was removed under reduced pressure and product was isolated by flash chromatography (90/10 chloroform/methanol). The resulting solid was triturated with hexanes. Product: white solid (19 mg, 0.061 mmol, 34% yield). ^{1}H NMR

(400 MHz, DMSO-d_6): δ 11.93 (s, NH, 1H), 8.82 (s, H-6, 1H), 7.85 (d, J=3.2 Hz, H-5″, 1H), 7.65 (d, J=3.2 Hz, H-4″, 1H), 6.21 (t, J=6.6 Hz, H-1′, 1H), 5.29 (d, J=4.4 Hz, 3′-OH, 1H), 5.01 (t, J=5.0 Hz, 5′-OH, 1H), 4.29–4.25 (m, H-3′, 1H), 3.88–3.86 (m, H-4′, 1H), 3.61–3.58 (m, H-5′, 2H), 2.23–2.19 (m, H-2′, 2H); ^{13}C NMR (100 MHz, DMSO-d_6): δ 161.3 (C-4), 158.1 (C-2″), 149.4 (C-2), 141.8 (C-4″), 138.5 (C-6), 119.8 (C-5″), 107.6 (C-5), 87.8 (C-4′), 85.3 (C-1′), 70.5 (C-3′), 61.3 (C-5′), 40.1 (C-2′); ESI-MS calcd for $C_{12}H_{13}N_3NaO_5S$ $[M+Na]^+$ 334.05, found 333.94; UV (buffer) λ_{max}=316 nm (ε=11,500).

4.1.6. 3′,5′-Di-*O*-acetyl-5-(fur-2-yl)-2′-deoxyuridine (10). To a solution of **1** (1.0 g, 3.5 mmol) in anhydrous pyridine (15 ml) was added acetic anhydride (825 μl, 891 mg, 8.73 mmol). The reaction was allowed to stir under argon at room temperature overnight. Solvent was removed under reduced pressure. Resulting oil was taken up in chloroform (200 ml) and washed with 1 M HCl (3×100 ml) and water (100 ml). The organic layer was dried over sodium sulfate and the solvent removed under reduced pressure. Product: light orange foam (1.34 g, 3.5 mmol, 99% yield). ^{1}H NMR (400 MHz, $CDCl_3$): δ 8.60 (s, NH, 1H), 7.97 (s, H-6, 1H), 7.32 (d, J=1.6 Hz, H-5″, 1H), 7.05 (d, J=3.2 Hz, H-3″, 1H), 6.45 (q, J=2 and 3.2 Hz, H-3″, 1H), 6.41 (td, J=5.6 and 8.8 Hz, H-1′, 1H), 5.28–5.26 (m, H-3′, 1H), 4.38–4.37 (m, H-5′, 2H), 4.29 (q, J=3 and 5 Hz, H-4′, 1H), 2.55–2.50 (m, H-2′, 1H), 2.28–2.19 (m, H-2′, 1H), 2.14 (s, Ac, 3H), 2.11 (s, Ac, 3H); ^{13}C NMR (100 MHz, CD_3Cl): δ 170.1 (Ac carbonyl), 170.0 (Ac carbonyl), 159.2 (C-4), 148.9 (C-2), 145.4 (C-2″), 140.9 (C-5″), 132.2 (C-6), 112.0 (C-4″), 109.7 (C-3″), 107.7 (C-5), 85.2 (C-4′), 82.5 (C-1′), 74.6 (C-3′), 64.1 (C-5′), 38.1 (C-2′), 21.0 (Ac methyl), 20.8 (Ac methyl); δ ESI-MS calcd for $C_{17}H_{19}N_2O_8$ $[M+H]^+$ 379.11, found 378.84 and for $C_{17}H_{18}N_2NNaO_8$ $[M+Na]^+$ 401.10, found 401.00.

4.1.7. 5-(Fur-2-yl)-2′-deoxycytidine (2). To a solution of **10** (800 mg, 2.1 mmol), 2,4,6-triisopropylbenzenesulfonyl chloride (2.0 g, 6.72 mmol), and 4-dimethylaminopyridine (825 mg, 6.72 mmol) in anhydrous acetonitrile (70 ml) was added triethylamine (937 μl, 680 mg, 6.72 mmol). The reaction was allowed to stir under argon at room temperature for 36 h. Once all starting material was consumed (monitored by TLC), concentrated ammonium hydroxide (90 ml) was added to the reaction flask. The reaction was again allowed to stir at room temperature overnight. Solvent was removed under reduced pressure. Resulting solid was taken up in cold chloroform and solid filtered off. Product: off white solid (590 mg, 2.0 mmol, 95% yield). ^{1}H NMR (400 MHz, DMSO-d_6): δ 8.25 (s, H-6, 1H), 7.68–7.67 (m, H-5″, 1H), 7.64 (br s, 4-NH_2, 1H), 6.65 (br s, 4-NH_2, 1H), 6.57–6.54 (m, H-4″ and H-3″, 2H), 6.16 (t, J=6.4 Hz, H-1′, 1H), 5.22 (d, J=4 Hz, 3′-OH, 1H), 5.08 (t, J=4.8 Hz, 5′-OH, 1H), 4.24–4.20 (m, H-3′, 1H), 3.80–3.78 (m, H-4′, 1H), 3.64–3.54 (m, H-5′, 2H), 2.20–2.15 (m, H-2′, 1H), 2.07–2.01 (m, H-2′, 1H); ^{13}C NMR (100 MHz, DMSO-d_6): δ 161.5 (C-4), 153.5 (C-2), 147.2 (C-2″), 142.3 (C-5″), 139.6 (C-6), 111.3 (C-4″), 106.5 (C-3″), 98.0 (C-5), 87.3 (C-4′), 85.2 (C-1′), 69.9 (C-3′), 60.9 (C-5′), 40.8 (C-2′); ESI-MS calcd for $C_{13}H_{16}N_3O_5$ $[M+H]^+$ 294.11, found 293.84; UV (buffer) λ_{max}=306 nm (ε=5000).

4.1.8. 8-(Fur-2-yl)-adenosine (3). To a suspension of **11** (208 mg, 0.6 mmol) and ammonium sulfate (43 mg) in anhydrous 1,1,1,3,3,3-hexamethyldisilazane (20 ml) was added anhydrous pyridine (2 ml). The reaction was refluxed under argon overnight. Solvent was removed under reduced pressure and the resulting oil was used without further purification. To a solution of the resulting trimethylsilyl protected nucleoside and dichlorobis(triphenylphosphine)-Pd(II) (28 mg, 0.04 mmol) in anhydrous tetrahydrofuran (10 ml) was added 2-(tributylstannyl)furan (950 μl, 1.0 g, 3.0 mmol) in a pressure tube and was heated to 90 °C for 24 h. Solvent was removed under reduced pressure and the resulting oil run through a silica plug with 5% methanol/dichloromethane. The resulting oil was taken up in methanol (5 ml) to which potassium carbonate (500 mg, 3.6 mmol) was added. The reaction was allowed to stir at room temperature overnight. Solid was filtered off and the product was recrystallized from methanol. Resulting white solid was run through a silica plug using 50/50 water/acetonitrile to remove any remaining potassium carbonate. Product: white solid (18.6 mg, 0.056 mmol, 9% yield). ^{1}H NMR (400 MHz, DMSO-d_6): δ 8.13 (s, H-2, 1H), 8.01 (d, J=2.4 Hz, H-5″, 1H), 7.58 (br s, 6-NH_2, 2H), 7.13 (d, J=4.8 Hz, H-3″, 1H), 6.77–6.76 (m, H-4″, 1H), 6.10 (d, J=8.8 Hz, H-1′, 1H), 5.77 (dd, J=4.4 and 12 Hz, 5′-OH, 1H), 5.46 (d, J=8.4 Hz, 2′-OH, 1H), 5.21 (d, J=5.6 Hz, 3′-OH, 1H), 5.14–5.08 (m, H-2′, 1H), 4.21–4.17 (m, H-3′, 1H), 3.98 (d, J=2.4 Hz, H-4′, 1H), 3.72–3.67 (m, H-5′, 1H), 3.51–3.49 (m, H-5′, 1H); ^{13}C NMR (100 MHz, DMSO-d_6): δ 156.3 (C-6), 152.3 (C-2), 149.6 (C-4), 145.6 and 143.3 (C-2″ and C-5″), 141.5 (C-8), 119.4 (C-5), 113.9 and 112.1 (C-3″ and C-4″), 89.3 (C-1′), 86.7 (C-4′), 71.6 (C-2′), 71.0 (C-3′), 62.2 (C-5′); ESI-MS calcd for $C_{14}H_{16}N_5O_5$ $[M+H]^+$ 334.12, found 334.02; UV (buffer) λ_{max}=304 nm (ε=18,000).

4.1.9. 8-(Fur-2-yl)-guanosine (4). To a suspension of **12** (139 mg, 0.4 mmol) and ammonium sulfate (21 mg) in anhydrous 1,1,1,3,3,3-hexamethyldisilazane (10 ml) was added anhydrous pyridine (1 ml). The reaction was stirred under argon and refluxed overnight. Solvent was removed under reduced pressure and the resulting oil was used without further purification. To a solution of the resulting trimethylsilyl protected nucleoside and dichlorobis(triphenylphosphine)Pd(II) (8.5 mg, 0.01 mmol) in anhydrous tetrahydrofuran (10 ml) was added 2-(tributylstannyl)furan (600 μl, 680 mg, 1.9 mmol) in a pressure tube and was heated to 90 °C for 24 h. Solvent was removed under reduced pressure and the resulting oil run through a silica plug with 5% methanol/dichloromethane. The resulting oil was taken up in methanol (5 ml) to which potassium carbonate (300 mg, 2.2 mmol) was added. The reaction was allowed to stir at room temperature overnight. Solid was filtered off and the product was recrystallized from methanol. Resulting white solid was run through a silica plug using 50/50 water/acetonitrile to remove any remaining potassium carbonate. Product: white solid (13.8 mg, 0.04 mmol, 10% yield). ^{1}H NMR (400 MHz, DMSO-d_6): δ 10.83 (s, 1-NH, 1H), 7.90 (d, J=1.6 Hz, H-5″, 1H), 6.94 (d, J=3.2 Hz, H-3″, 1H), 6.68 (q, J=1.7 Hz, H-4″, 1H), 6.46 (br s, 2-NH_2, 2H), 5.91 (d, J=6.4 Hz, H-1′, 1H), 5.38 (d, J=6.0 Hz, 2′-OH, 1H), 5.04–4.96 (m, 3′-OH, 5′-OH, and H-2′, 3H), 4.13–4.08 (m, H-3′, 1H), 3.84 (dt, J=4.8 and 8.8 Hz, H-4′, 1H), 3.68–3.63 (m, H-5′, 1H), 3.54–3.48 (m, H-5′, 1H);

^{13}C NMR (100 MHz, DMSO-d_6): δ 156.5 (C-6), 153.3 (C-2), 151.7 (C-4), 144.4 and 143.9 (C-2″ and C-5″), 138.2 (C-8), 117.3 (C-5), 112.1 and 111.7 (C-3″ and C-4″), 89.0 (C-1′), 85.7 (C-4′), 70.6 and 70.5 (C-2′ and C-3′), 62.1 (C-5′); ESI-MS calcd for $C_{14}H_{16}N_5O_6$ $[M+H]^+$ 350.11, found 349.80; UV (buffer) λ_{max}=294 nm (ε=16,000).

4.1.10. 5′-Dimethoxytrityl-5-(fur-2-yl)-2′-deoxyuridine (13). To a solution of **1** (163 mg, 0.554 mmol) and 4,4′-dimethoxytrityl chloride (226 mg, 0.669 mmol) in anhydrous pyridine (3 ml) was added triethylamine (60 μl). The reaction was stirred at room temperature under argon for 8 h and evaporated under reduced pressure. The product was purified by flash column chromatography (1/1 ethyl acetate/hexanes, 1% Et_3N). Product: light brown foam (234 mg, 0.393 mmol, 71% yield). ^{1}H NMR (400 MHz, DMSO-d_6): δ 11.70 (s, NH, 1H), 7.96 (s, H-6, 1H), 7.27–7.16 (m, DMT and H-5″, 10H), 6.84–6.81 (m, DMT and H-3″, 5H), 6.46–6.44 (m, H-4″, 1H), 6.18 (t, J=6.6 Hz, H-1′, 1H), 5.36 (d, J=4.4 Hz, 3′-OH, 1H), 4.23–4.19 (m, H-3′, 1H), 3.96–3.93 (m, H-4′, 1H), 3.69 (s, DMT-OCH_3, 6H), 3.24–3.15 (m, H-5′, 2H), 2.27–2.24 (m, H-2′, 2H); ^{13}C NMR (100 MHz, DMSO-d_6): δ 160.1, 158.0, 149.3, 146.1, 144.7, 141.2, 135.5, 133.9, 129.6, 127.7, 127.6, 126.6, 113.1, 111.4, 107.9, 105.6, 85.8, 85.1, 70.3, 63.6, 55.0, 40.2; ESI-MS calcd for $C_{34}H_{32}N_2NaO_8$ $[M+Na]^+$ 619.21, found 619.08.

4.1.11. 3′-(2-Cyanoethyl)diisopropylphosphoramidite-5′-dimethoxytrityl-5-(fur-2-yl)-2′-deoxyuridine (14). Compound **13** was taken up in anhydrous acetonitrile and solvent was removed under reduced pressure (5×). To a solution of **13** (58 mg, 0.10 mmol) and 1-*H* tetrazole (0.45 M solution in acetonitrile: 215 μl, 0.097 mmol) in anhydrous acetonitrile (2 ml) was added 2-cyanoethyl tetraisopropylphosphorodiamidite (37 μl, 35 mg, 0.12 mmol). The solution was stirred at room temperature under argon for 4 h. The reaction mixture was diluted with cold 1% triethylamine/dichloromethane (100 ml) and washed with 1 M $NaHCO_3$ (2×10 ml) and brine (2×10 ml). The organic layer was dried over sodium sulfate and evaporated under reduced pressure. The product was purified by flash column chromatography (1/1 ethyl acetate/hexanes, 1% Et_3N). Product: light brown foam (50 mg, 0.063 mmol, 65% yield). ^{1}H NMR (400 MHz, DMSO-d_6): δ 11.60 (s, NH, 1H), 7.99 (s, H-6, 1H), 7.39–7.17 (m, DMT and H-5′, 10H), 6.82–6.79 (m, DMT and H-3′, 5H), 6.45–6.43 (m, H-4″, 1H), 6.17 (t, J=6.4 Hz, H-1′, 1H), 4.50–4.44 (m, H-3′, 1H), 4.11–4.08 (m, H-4′, 1H), 3.69–3.39 (m, DMT-OCH_3, isopropyl and cyanoethyl, 10H), 3.24–3.19 (m, H-5′, 2H), 2.64–2.61 (m, cyanoethyl, 2H), 2.46–2.34 (m, H-2′, 2H), 1.23–1.08 (m, isopropyl, 12H); ^{13}C NMR (100 MHz, DMSO-d_6): δ 160.1, 158.1, 149.2, 146.1, 144.6, 141.2, 135.3, 134.0, 129.7, 127.7, 127.6, 126.6, 118.7, 113.1, 111.5, 108.0, 105.7, 85.9, 85.2, 72.3, 63.5, 58.5, 55.0, 42.6, 42.5, 40.2, 24.3, 24.3, 24.2, 19.8; ^{31}P NMR (162 MHz, DMSO-d_6, referenced to H_3PO_4): δ 148.7, 148.3; ESI-MS calcd for $C_{43}H_{49}N_4NaO_9P$ $[M+Na]^+$ 819.31, found 819.14.

4.2. Oligonucleotide synthesis

4.2.1. Oligonucleotide synthesis and purification. Unmodified oligonucleotides were purchased from Intergraded DNA Technologies (Coralville, Iowa) and purified by PAGE as described below. Modified oligonucleotides were synthesized on a 1.0 μmol scale (500 Å CPG column) using a Biosearch Cyclone Plus DNA synthesizer. Phosphoramidite **14** was site specifically incorporated into the oligonucleotides by trityl-off synthesis of the base oligonucleotide, followed by manual coupling of phosphoramidite **14**. Typically, the modified phosphoramidite was dissolved in 100 μl of anhydrous acetonitrile to give a final concentration of 0.1 M. The phosphoramidite solution was pushed into the CPG column via syringe and then 200 μl of 0.45 M 1*H*-tetrazole was pushed into the other end of the column via syringe. Coupling reactions were allowed to proceed for 2–3 min (88% unoptimized coupling efficiency) and were subsequently followed by standard oxidation and capping steps. The rest of the oligonucleotide was synthesized via the standard trityl-off procedure. Upon completion of the oligonucleotide synthesis, the CPG column was treated with 3 ml of 30% aqueous ammonium hydroxide for 2 h at room temperature, mixing via syringe every 1 h. The resulting solution was removed and the CPG column was treated with 1 ml of 30% aqueous ammonium hydroxide at room temperature for 15 min, mixing via syringe every 5 min. The resulting aqueous ammonium hydroxide solutions were consolidated and stored at room temperature for 24 h. The aqueous ammonium hydroxide solutions were freeze-dried and purified by 20% polyacrylamide gel electrophoresis. The oligonucleotide was visualized by UV shadowing, bands were excised from the gel, and extracted with 1× TBE buffer for 36 h. The resulting solution was filtered (Bio-Rad poly-prep chromatography column) and desalted using a Sep-Pak cartridge (Waters Corporation, MA). The following 260 nm extinction coefficients were used to determine concentration of oligonucleotides: dG=11,700, dC=7300, dA=15,400, dT=8800, and **1**=13,000.

4.2.2. Oligonucleotide sequencing using MALDI-TOF MS. The MW of each control and modified oligonucleotide was determined via MALDI-TOF MS. One microliter of 200 μM stock solution of each oligonucleotide was combined with 1 μl of ammonium citrate buffer (PE Biosystems), 1 μl of 75 μM DNA standard (5′-GCTGAA TACATAAGACG-3′), and 6 μl of saturated 3-hydroxypiccolinic acid. The samples were desalted with an ion-exchange resin (PE Biosystems) and spotted onto a gold-coated MALDI plate where they were dried on a 55 °C heat block. The resulting spectra were calibrated relative to the +1 and +2 ions of the internal DNA standard, thus the observed oligonucleotides should have a resolution of ±2 mass units. Modified oligonucleotide **15** was sequenced via onplate digestion (Sequazyme Oligonucleotide Sequencing Kit—Applied Biosystems). Two microliters of water and 1 μl of 200 μM stock solution of oligonucleotide **15** were combined and spotted eight times onto a gold-coated MALDI plate. Two microliters of SVP dilutions (1 μl of ammonium citrate buffer and 1 μl of SVP dilution) were added to the first five wells and 2 μl of BSP dilutions (1 μl of BSP reaction buffer and 1 μl of BSP dilution) were added to the remaining three wells. The MALDI plate was incubated in a humidity chamber (Applied Biosystems) at 37 °C for 20 min. Seven microliters of saturated 3-hydroxypiccolinic acid was

added to each well. The samples were desalted with an ion-exchange resin (PE Biosystems) and then respotted onto the same wells of the gold-coated MALDI plate where they were subsequently dried on a 55 °C heat block. All MALDI-TOF spectra were collected on a PE Biosystems Voyager-DE STR MALDI-TOF spectrometer in positive-ion, delayed-extraction mode. The following nucleoside masses were used to confirm the sequence: dG=329.053, dC=289.046, dA=313.058, dT=304.046, and the modified furan dT=356.041.

4.3. UV and fluorescence studies

4.3.1. Thermal denaturation studies. All hybridizations and UV melting experiments were carried out in 100 mM sodium chloride, 10 mM sodium phosphate buffer at pH 7.0 using a Beckman-Coulter DU® 640 spectrometer with a high performance temperature controller and micro auto six holder. Samples (double-stranded concentrations: 1 μM) were heated to 95 °C for 5 min and cooled to room temperature over 2–3 h prior to measurements. Samples were placed in a stoppered 1.0-cm path length cell and a background spectra (buffer) was subtracted from each sample. Denaturation runs were performed between 26 and 75 °C at a scan rate of 0.5 °C min^{-1} with optical monitoring every minute at 260 nm. Beckman-Coulter software (provided with T_m Analysis Accessory for DU® Series 600 Spectrometers) determined the melting temperatures utilizing the first derivative from the melting profile.

4.3.2. Steady-state fluorescence and absorption spectra. Steady-state fluorescence experiments were carried out at ambient temperature (unless otherwise noted) in a micro fluorescence cell with a path length of 1.0 cm (Hellma GmbH & Co. KG, Müllheim, Germany) on a Perkin–Elmer LS 50B luminescence spectrometer (Figs. 4–7 and 13) or a Horiba fluoromax-3 luminescence spectrometer (Figs. 2 and 14). All nucleoside samples were measured at specified concentrations (≤1% DMSO) in the appropriate spectroscopic grade solvent.

4.3.3. Temperature dependent fluorescence spectra. Temperature dependent fluorescence experiments were carried out at 10° intervals from 25 to 75 °C in a micro fluorescence cell with a path length of 1.0 cm (Hellma GmbH & Co. KG, Müllheim, Germany) using a temperature controlled cell holder connected to an external water-based temperature control unit on a Perkin–Elmer LS 50B luminescence spectrometer. Nucleoside samples were measured at 1.0×10^{-5} M (**1** and **2**) and 1.0×10^{-6} M (**3** and **4**) in water (≤1% DMSO). Spectra at the appropriate temperature were recorded after allowing the sample to equilibrate for 14 min.

4.4. X-ray structures

Suitable crystals for nucleosides **1**, **2**, **6**, **8**, and **9** were obtained from slow diffusion of chloroform into a methanol solution containing the nucleoside.

Crystal structures for **1** and **6** match previously published unit cell and space group data.[57,58]

Crystal	**2**	**8**	**9**
Empirical formula	$C_{13}H_{15}N_3O_5$	$C_{12}H_{14}N_3O_{6.5}$	$C_{12}H_{13}N_3O_5S$
M (g mol^{-1})	293.28	296.26	311.31
Crystal system	Orthorhombic	Triclinic	Monoclinic
Space group	$P2(1)2(1)2(1)$	P1	$P2(1)$
a (Å)	4.5420(2)	6.6557(13)	5.9563(7)
b (Å)	10.2410(4)	10.1584(19)	20.591(3)
c (Å)	26.9210(10)	10.397(2)	10.3793(11)
β (°)	90	83.596(3)	90.762(9)
V ($Å^3$)	1252.22(9)	633.7(2)	1272.9(3)
Z	4	2	4, 2
T (K)	100(2)	100(2)	100(2)
λ (Å)	0.71073	0.71073	1.54178
D_{calcd} (g cm^{-3})	1.556	1.595	1.624
μ (mm^{-1})	0.121	0.132	2.544
Reflections collected	8150	5352	4450
Independent reflections	2850	4786	2785
Observed data [$I>2(\sigma)I$]	2850	4786	2785
Final R_1, wR^2 (obsd data)	0.0439, 0.1126	0.0326, 0.0842	0.0454, 0.1048
Final R_1, wR^2 (all data)	0.0441, 0.1129	0.0334, 0.0856	0.0571, 0.1114
ρ_{min}, ρ_{max} (e $Å^{-3}$)	−0.444, 0.744	−0.269, 0.327	−0.362, 0.320

Crystallographic data (excluding structure factors) for compounds **1**, **2**, **6**, **8**, and **9** in this paper have been deposited with the Cambridge Crystallographic Data Centre as supplementary publication numbers CCDC 627723, 627722, 627725, 627724, and 632875, respectively. Copies of the data can be obtained, free of charge, on application to CCDC, 12 Union Road, Cambridge CB2 1EZ, UK (fax: +44 (0)1223 336033 or e-mail: deposit@ccdc.cam.ac.uk).

Acknowledgements

We thank the National Institutes of Health (GM069773) for generous support, Dr. Kenneth F. Blount for his generous and critical help with the MALDI-TOF experiments, and the UCSD small molecule X-ray facility for determination of X-ray structures.

References and notes

1. Daniels, M.; Hauswirth, W. *Science* **1971**, *171*, 675–677.
2. Morgan, J. P.; Daniels, M. *Photochem. Photobiol.* **1980**, *31*, 207–213.
3. Wilson, R. W.; Callis, P. R. *Photochem. Photobiol.* **1980**, *31*, 323–327.
4. Callis, P. R. *Annu. Rev. Phys. Chem.* **1983**, *34*, 329–357.
5. Albinsson, B.; Norden, B. *J. Am. Chem. Soc.* **1993**, *115*, 223–231.
6. Andreasson, J.; Holmén, A.; Albinsson, B. *J. Phys. Chem. B* **1999**, *103*, 9782–9789.
7. Pecourt, J. M. L.; Peon, J.; Kohler, B. *J. Am. Chem. Soc.* **2000**, *122*, 9348–9349.
8. Nir, E.; Kleinermanns, K.; Grace, L.; de Vries, M. S. *J. Phys. Chem. A* **2001**, *105*, 5106–5110.
9. Onidas, D.; Markovitsi, D.; Marguet, S.; Sharonov, A.; Gustavsson, T. *J. Phys. Chem. B* **2002**, *106*, 11367–11374.
10. Ward, D. C.; Reich, E.; Stryer, L. *J. Biol. Chem.* **1969**, *244*, 1228–1237.
11. Wu, P. G.; Nordlund, T. M.; Gildea, B.; Mclaughlin, L. W. *Biochemistry* **1990**, *29*, 6508–6514.
12. Singleton, S. F.; Shan, F.; Kanan, M. W.; McIntosh, C. M.; Stearman, C. J.; Helm, J. S.; Webb, K. J. *J. Org. Lett.* **2001**, *3*, 3919–3922.

13. Hawkins, M. E. *Cell Biochem. Biophys.* **2001**, *34*, 257–281.
14. Secrist, J. A.; Barrio, J. R.; Leonard, N. J. *Science* **1972**, *175*, 646–647.
15. Holmén, A.; Albinsson, B.; Nordén, B. *J. Phys. Chem.* **1994**, *98*, 13460–13469.
16. Godde, F.; Toulmé, J. J.; Moreau, S. *Biochemistry* **1998**, *37*, 13765–13775.
17. Arzumanov, A.; Godde, F.; Moreau, S.; Toulmè, J. J.; Weeds, A.; Gait, M. J. *Helv. Chim. Acta* **2000**, *83*, 1424–1436.
18. Wilhelmsson, L. M.; Holmén, A.; Lincoln, P.; Nielsen, P. E.; Nordén, B. *J. Am. Chem. Soc.* **2001**, *123*, 2434–2435.
19. Loakes, D.; Brown, D. M.; Salisbury, S. A.; McDougall, M. G.; Neagu, C.; Nampalli, S.; Kumar, S. *Helv. Chim. Acta* **2003**, *86*, 1193–1204.
20. Engman, K. C.; Sandin, P.; Osborne, S.; Brown, T.; Billeter, M.; Lincoln, P.; Nordén, B.; Albinsson, B.; Wilhelmsson, L. M. *Nucleic Acids Res.* **2004**, *32*, 5087–5095.
21. Gao, J.; Liu, H.; Kool, E. T. *J. Am. Chem. Soc.* **2004**, *126*, 11826–11831.
22. Liu, H.; Gao, J.; Maynard, L.; Saito, Y. D.; Kool, E. T. *J. Am. Chem. Soc.* **2004**, *126*, 1102–1109.
23. Lu, H.; He, K.; Kool, E. T. *Angew. Chem., Int. Ed.* **2004**, *43*, 5834–5836.
24. Lee, A. H.; Kool, E. T. *J. Org. Chem.* **2005**, *70*, 132–140.
25. Liu, H.; Gao, J.; Kool, E. T. *J. Am. Chem. Soc.* **2005**, *127*, 1396–1402.
26. Liu, H.; Gao, J.; Kool, E. T. *J. Org. Chem.* **2005**, *70*, 639–647.
27. Sandin, P.; Wilhelmsson, L. M.; Lincoln, P.; Powers, V. E.; Brown, T.; Albinsson, B. *Nucleic Acids Res.* **2005**, *33*, 5019–5025.
28. Lee, A. H.; Kool, E. T. *J. Am. Chem. Soc.* **2006**, *128*, 9219–9230.
29. Ren, R. X. F.; Chaudhuri, N. C.; Paris, P. L.; Rumney, S.; Kool, E. T. *J. Am. Chem. Soc.* **1996**, *118*, 7671–7678.
30. Coleman, R. S.; Madaras, M. L. *J. Org. Chem.* **1998**, *63*, 5700–5703.
31. Brauns, E. B.; Madaras, M. L.; Coleman, R. S.; Murphy, C. J.; Berg, M. A. *J. Am. Chem. Soc.* **1999**, *121*, 11644–11649.
32. Coleman, R. S.; Pires, R. M. *Nucleosides Nucleotides* **1999**, *18*, 2141–2146.
33. Strässler, C.; Davis, N. E.; Kool, E. T. *Helv. Chim. Acta* **1999**, *82*, 2160–2171.
34. Brauns, E. B.; Madaras, M. L.; Coleman, R. S.; Murphy, C. J.; Berg, M. A. *Phys. Rev. Lett.* **2002**, *88*, 158101-1–158101-4.
35. Coleman, R. S.; Mortensen, M. A. *Tetrahedron Lett.* **2003**, *44*, 1215–1219.
36. Gearheart, L. A.; Somoza, M. M.; Rivers, W. E.; Murphy, C. J.; Coleman, R. S.; Berg, M. A. *J. Am. Chem. Soc.* **2003**, *125*, 11812–11813.
37. Andreatta, D.; Perez Lustres, J. L.; Kovalenko, S. A.; Ernsting, N. P.; Murphy, C. J.; Coleman, R. S.; Berg, M. A. *J. Am. Chem. Soc.* **2005**, *127*, 7270–7271.
38. Andreatta, D.; Sen, S.; Perez Lustres, J. L.; Kovalenko, S. A.; Ernsting, N. P.; Murphy, C. J.; Coleman, R. S.; Berg, M. A. *J. Am. Chem. Soc.* **2006**, *128*, 6885–6892.
39. Netzel, T. L.; Zhao, M.; Nafisi, K.; Headrick, J.; Sigman, M. S.; Eaton, B. E. *J. Am. Chem. Soc.* **1995**, *117*, 9119–9128.
40. Kerr, C. E.; Mitchell, C. D.; Headrick, J.; Eaton, B. E.; Netzel, T. L. *J. Phys. Chem. B* **2000**, *104*, 1637–1650.
41. Seela, F.; Zulauf, M.; Sauer, M.; Deimel, M. *Helv. Chim. Acta* **2000**, *83*, 910–927.
42. Seela, F.; Feiling, E.; Gross, J.; Hillenkamp, F.; Ramzaeva, N.; Rosemeyer, H.; Zulauf, M. *J. Biotechnol.* **2001**, *86*, 269–279.
43. Hurley, D. J.; Seaman, S. E.; Mazura, J. C.; Tor, Y. *Org. Lett.* **2002**, *4*, 2305–2308.
44. McKeen, C. M.; Brown, L. J.; Nicol, J. T.; Mellor, J. M.; Brown, T. *Org. Biomol. Chem.* **2003**, *1*, 2267–2275.
45. Kawai, R.; Kimoto, M.; Ikeda, S.; Mitsui, T.; Endo, M.; Yokoyama, S.; Hirao, I. *J. Am. Chem. Soc.* **2005**, *127*, 17286–17295.
46. Ranasinghe, R. T.; Brown, T. *Chem. Commun.* **2005**, 5487–5502.
47. Leroy, E.; Lami, H.; Laustria, G. *Photochem. Photobiol.* **1971**, *13*, 411–421.
48. Pelter, A.; Rowlands, M.; Clements, G. *Synthesis* **1987**, 51–53.
49. It has been shown that conjugation of a thiophene or thiazole moiety to the 6-position of guanosine results in highly fluorescent nucleoside analogues, for details see: Mitsui, T.; Kimoto, M.; Kawai, R.; Yokoyama, S.; Hirao, I. *Tetrahedron*, in press. doi:10.1016/j.tet.2006.11.096
50. Wigerinck, P.; Pannecouque, C.; Snoeck, R.; Claes, P.; Declercq, E.; Herdewijn, P. *J. Med. Chem.* **1991**, *34*, 2383–2389.
51. Gutierrez, A. J.; Terhorst, T. J.; Matteucci, M. D.; Froehler, B. C. *J. Am. Chem. Soc.* **1994**, *116*, 5540–5544.
52. The ribose forms of adenosine and guanosine were used due to their commercial availability.
53. Persson, T.; Gronowitz, S.; Hornfeldt, A. B.; Johansson, N. G. *Bioorg. Med. Chem.* **1995**, *3*, 1377–1382.
54. Reichardt, C. *Chem. Rev.* **1994**, *94*, 2319–2358.
55. Tinsley, R. A.; Walter, N. G. *RNA* **2006**, *12*, 522–529.
56. Adequate fluorescence readings also depend upon the sensitivity of the luminescence spectrometer.
57. Creuven, I.; Evrard, C.; Olivier, A.; Evrard, G.; VanAerschot, A.; Wigerinck, P.; Herdewijn, P.; Durant, F. *Antiviral Res.* **1996**, *30*, 63–74.
58. Creuven, I.; Norberg, B.; Oliver, A.; Evrard, C.; Evrard, G.; Wigerinck, P.; Herdewijn, P.; Durant, F. *J. Chem. Crystallogr.* **1996**, *26*, 777–789.